Polymer 54 (2013) 981–994

Contents lists available at SciVerse ScienceDirect

Polymer

journal homepage: www.elsevier.com/locate/polymer

Feature article

Recent progress in the use of photoirradiation in living radical polymerization

Shigeru Yamago [a,b,*], Yasuyuki Nakamura [a,b]

[a] Institute for Chemical Research, Kyoto University, Uji 611-0011, Kyoto, Japan
[b] CREST, Japan Science and Technology Agency, Tokyo 102-0076, Japan

ARTICLE INFO

Article history:
Received 7 October 2012
Received in revised form
9 November 2012
Accepted 15 November 2012
Available online 8 December 2012

Keywords:
Living radical polymerization
Photoirradiation
Precision polymer synthesis

ABSTRACT

The effects of photoirradiation in controlled and living radical polymerization (LRP), namely nitroxide-mediated polymerization (NMP), atom-transfer radical polymerization (ATRP), cobalt-mediated radical polymerization (CMRP), reversible addition-fragmentation chain transfer polymerization (RAFT), organoiodine-mediated radical polymerization (IRP), and organotellurium-mediated radical polymerization (TERP), are summarized. As in the conventional radical polymerization, photoirradiation has been used for generating radicals under mild conditions in LRP methods. In addition to this use, photoirradiation is also used to overcome the difficulties characteristic to each method, such as activation of catalysis, generation of controlling agents, and increasing the polymer-end structure. The most-recent developments in the use of photochemistry in LRP are summarized in this review.

1. Introduction

Radical polymerization is one of the most important industrial polymerization technologies, and 40–45% of all synthetic polymers are estimated to be produced by this method [1]. This is primarily because of the robustness of this method, which originates from the neutral and highly reactive character of radicals. Polymerization proceeds with a variety of monomer families and is compatible with various polar functional groups and solvents, including water [2–6]. These conditions are in sharp contrast to other vinyl polymerization methods, namely, anionic, cationic, and coordination polymerizations, which require stringent reaction conditions to avoid the occurrence of undesirable side reactions involving protic solvents, oxygen, and/or polar functional groups.

The disadvantage of conventional radical polymerization, however, is insufficient control of the macromolecular structure, resulting in macromolecules that are polydisperse with a broad molecular weight distribution (MWD). Controlled and living radical polymerization (LRP) methods have been developed primarily to overcome this difficulty in controlling molecular weights and MWDs. In addition, LRP also creates the new possibility of controlling the monomer sequence through block copolymer synthesis and synthesizing end-functional polymers by selective transformation of the living polymer-ends. Therefore, LRP is now widely used on the bench scale for the synthesis of new polymeric materials with improved and/or new properties and functions, and its industrial applications have been rapidly progressing [7].

LRPs that have been widely used include nitroxide-mediated radical polymerization (NMP) [8,9], atom-transfer radical polymerization (ATRP) [10–15], and reversible addition-fragmentation chain transfer radical polymerization (RAFT) [16–19]. Organotellurium- [20–22], organostibine- [23–25], and organobismuthine-mediated LRP [26,27] (SBRP, BIRP, and TERP, respectively) [28–32] are relatively new methods developed by the author's research group. New variants of LRP have also emerged, such as cobalt-mediated polymerization [33–36], titanium-catalyzed polymerization [37], and single-electron transfer LRP [38,39]. Organoiodine-mediated LRP (IRP), which is one of the oldest LRP [40–42], has been also used in many instances.

LRP relied on reversible generation of the polymer-end radical $P\cdot$ from a dormant species P–X, which possesses appropriate functional group X at the polymer-end for radical generation (Scheme 1) [14,43]. This pseudo deactivation of the polymer-end radical to the dormant species decreases the concentration of the radical species in solution and minimizes undesirable side reactions leading to dead polymers. Therefore, the activity of polymer-end radical species is preserved throughout the polymerization period as a form of dormant species. Furthermore, the rapid deactivation makes it possible to elongate all of the polymer chains

* Corresponding author. Institute for Chemical Research, Kyoto University, Uji 611-0011, Kyoto, Japan.
E-mail address: yamago@scl.kyoto-u.ac.jp (S. Yamago).

0032-3861/$ – see front matter © 2012 Elsevier Ltd. All rights reserved.
http://dx.doi.org/10.1016/j.polymer.2012.11.046

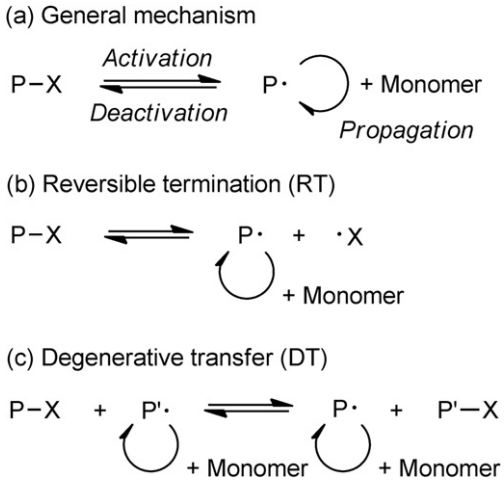

Scheme 1. Activation and deactivation mechanism of dormant (P–X and P'–X) and polymer-end radical species ($P\cdot$ and $P'\cdot$), respectively, in living radical polymerization.

with similar chain lengths giving structurally well-controlled polymers with narrow MWD. The term "living" will be used throughout this manuscript when these criteria are fulfilled, despite the IUPAC recommends use of "reversible-deactivation radical polymerization" for this type of polymerization because the termination reaction of polymer-end radicals cannot be completely inhibited [44].

There are two activation/deactivation mechanisms of the dormant/radical species. One is reversible termination (RT) shown in Scheme 1b, in which homolytic cleavage of the P–X bond in the dormant species generates polymer-end radical $P\cdot$(P denotes polymer here) and persistent radical $\cdot X$. The selective recombination of $P\cdot$ and $\cdot X$ radicals is controlled by the persistent radical effect [45]. The other mechanism is degenerative chain transfer (DT) shown in Scheme 1c, in which polymer-end radical $P'\cdot$(P' denotes polymer having either same or different chain length with P) undergoes a homolytic substitution reaction with dormant species P–X, generating new radical $P\cdot$and new dormant species P'–X.

The chemical structure of X and the activation/deactivation mechanisms of the dormant/radical species make each LRP method unique, both mechanistically and synthetically. NMP and ATRP exclusively proceed by the RT mechanism, and RAFT proceeds by the DT mechanism. TERP, SBRP, BIRP, and IRP predominantly proceed via the DT mechanism, but RT also contributes to a small extent. CMRP also proceeds by both RT and DT depending on the conditions, but RT plays a more important role than DT for the MWD control.

Various physical and chemical stimuli, such as heat, metal catalysts, and free-radical initiators, have been used to realize efficient activation/deactivation and control of the molecular weight and MWD. Photochemical stimuli have been widely employed in conventional radical polymerization as a key technique in various applications, such as coatings, adhesives, microelectronics, and so forth [46,47], and the use of photochemistry in the control of radical polymerization has also emerged since the pioneering work on the invention of photoiniferter (initiator-transfer agent-termination) [48–50]. Otsu and coworkers reported photopolymerization in the presence of dithiocarbamate, such as **1**, showing living character, including a linear increase in molecular weight upon monomer conversion and successful synthesis of block copolymers. The mechanism of iniferter is identical to the RT mechanism shown in Scheme 1b, in which homolytic C–S bond cleavage of **1** by photoirradiation generates a transient benzyl radical and dithiocarbamyl

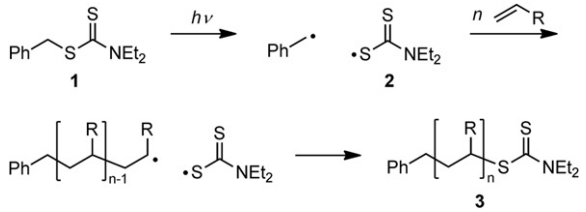

Scheme 2. Controlled polymerization using "photoiniferter".

radical **2** (Scheme 2). After propagation with the monomer, the polymer-end radical reacts with **2** giving dormant species **3** having a dithiocarbamate group at the polymer-end. However, this method is not a living system and gives polymers with a broad MWD. This is because dithiocarbamates are poor chain transfer agents (CTAs) and because **2** is not a persistent radical and initiates a new polymer chain. Kwon and coworkers utilized diphenyl diselenide and organoselenium compounds as photoiniferters, but sufficient control could not be attained for the same reason as that mentioned above with respect to dithiocarbamate [51–53].

This review focuses on the use of photoirradiation in LRP [54,55]. The major motivation to utilize photochemistry is to enable LRP to proceed under mild thermal conditions by activating the dormant species at low temperature. In addition, photochemistry has been utilized to overcome the difficulties particular to each LRP method. Therefore, photoirradiation is used not only for generating initiating radical species as in conventional photopolymerization, but also for other purposes, such as activation of catalysis, generation of controlling agents, and increasing the polymer-end structure. The most-recent developments in the use of photochemistry in LRP are summarized in this review.

2. Photo-induced LRP

2.1. Photo-induced NMP

The conventional NMP relies on the thermal homolysis of an alkoxyamine dormant species, generating a polymer-end radical and a persistent nitroxyl radical (Scheme 3). The major drawback is the high temperature required for the activation of dormant species. This condition is unattractive for monomers having low thermal stability and low ceiling temperature. Furthermore, since the activation of dormant species having strong oxygen-carbon bonds, such as polyacrylate polymer-ends, is difficult, polymerizable monomer families are quite limited. This problem has been partly solved by the invention of bulky nitoxides, such as TIPNO [56], DEPN [57], and hydroxyl- and siloxy-substituted TEMPO derivatives [58], enabling acrylate polymerization in a controlled manner. However, the polymerization still requires a high temperature, such as heating at 90 °C. Photochemical activation of the dormant species would enable polymerization at a lower temperature.

The first work towards the photochemical NMP was reported by Scaiano and coworkers in 1997 [59]. They found that TEMPO-derived alkoxyamines were activated by photosensitization from either the triplet excited state of xanthone or the singlet excited state

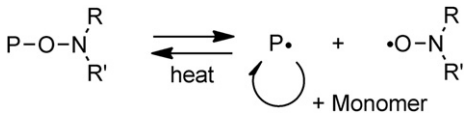

Scheme 3. Activation/deactivation mechanism in NMP.

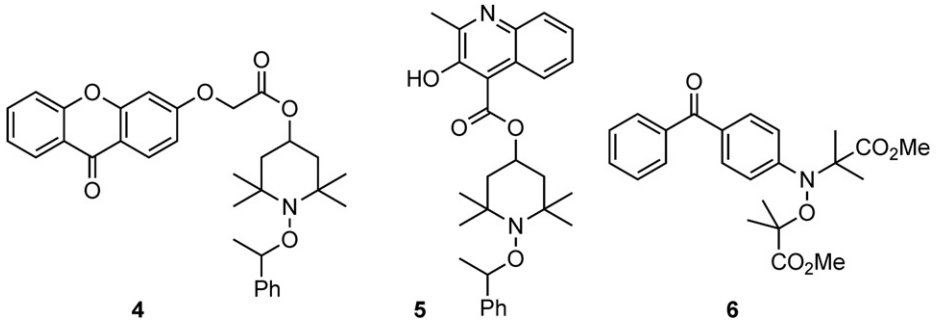

Scheme 4. Structures of alkoxyamines directly connected chromophores.

of pyrene, generating the corresponding carbon-centered radicals and TEMPO. However, polymerization reaction was not investigated due to the low efficiency in generating the carbon-centered radicals. Photo-induced NMP has been examined using several alkoxyamines, in which nitroxide moiety was tethered with chromophore (Scheme 4). Photopolymerization of methyl methacrylate (MMA), styrene (St), and butyl acrylate (BA) proceeded at room temperature by using these alkoxyamines, but control of M_n and MWD was insufficient in all cases.

Neckers and coworkers synthesized TEMPO-xanthone hybrid alkoxyamine **4** [60]. The generation of a carbon-centered radical from **4** could not be detected, but it served as a photoinitiator in MMA polymerization. A linear increase in the number average molecular weight (M_n) was observed up to high molecular weight ($>8 \times 10^5$). However, the polymer-end became inert after the polymerization, and the result is consistent with the fact that nitroxide radical undergoing β-hydrogen abstraction of the MMA-polymer-end radical giving a dead polymer [61,62]. Therefore, the system was not living.

Scaiano and coworkers reported that alkoxyamine **5**, in which 2-methyl-3-hydroxy quinoline is tethered to TEMPO, efficiently and reversibly generated 2-phenylethyl radical and the corresponding nitroxyl radical upon photoirradiation via energy transfer from photoexcited quinoline to the hydroxylamine moiety [63]. However, its applications to LRP are limited, because polymerization of St in the presence of **5** under photoirradiation afforded PSt with low M_n (2700) and a broad MWD ($M_w/M_n = 1.60$, where M_w refers to the weight average molecular weight).

Guillaneuf and coworkers designed alkoxyamine **6**, in which benzophenene moiety is directly connected to the nitrogen of hydroxylamine [64]. Photolysis of **6** led not only to the desired C–O bond cleavage but also to O–N bond cleavage, but it was used so far as a photoinitiator in BA polymerization. M_n increased nearly linearly with monomer conversion, and the polymer-end was living on the basis of a chain extension test. However, M_ns deviated significantly from the theoretical values, and the MWDs were broad ($M_w/M_n > 2$) throughout the polymerization period.

2.2. Photo-induced ATRP

The activation mechanism of ATRP involves the reduction of organohalide dormant species, typically organobromides and organochlorides, by low-valent metal catalyst ML_n (L refers to ligand), generating a polymer-end radical and oxidized metal species MXL_n, which serves as a persistent radical equivalent (Scheme 5). Halogen abstraction of the polymer-end radical from MXL_n is the deactivation mechanism. MXL_n accumulates at the initial stage of polymerization according to the persistent radical effect. Ligand-modified copper and ruthenium are among the most common catalysts, but other metals, such as iron, nickel, palladium, and so forth, have also been used. Due to the operational simplicity and the ease of availability of initiators, metals, and ligands, ATRP has been widely used in the controlled synthesis of polymer materials. However, the requirement for metal catalysts not only causes coloration but also involves the risk of toxicity of the resulting polymer materials.

A precursor to activator regenerated by electron transfer (ARGET) ATRP [65,66] and initiators for continuous activator regeneration (ICAR) ATRP [67] have been developed to decrease the catalyst loading (Scheme 6). ARGET ATRP relies on regeneration of an active, low-valent metal catalyst by a reducing agent from an inactive, high valent metal catalyst that accumulates as polymerization proceeds. Various reducing agents, as exemplified by tin(II) 2-ethylhexanoate, glucose, and ascorbic acid have been successfully employed [68]. ICAR utilizes a carbon-centered radical generated from an azo-initiator as a reducing agent of the high valent metal species, and the reaction generates an ATRP initiator having a carbon–halogen bond. Electrochemical generation of active catalyst [69] and single-electron transfer LRP [39] have been recently developed to decrease the metal catalyst loading. With this approach, the nearly stoichiometric amount of catalyst (~1000 ppm) over an organohalogen initiator required in conventional ATRP has been reduced by two orders of magnitude to ~10 ppm (~0.002 equivalent over the initiator) or even less under the new conditions.

One motivation for utilizing photoirradiation is to decrease the catalyst loading by increasing the reactivity of the metal catalyst. The effect of light in ATRP was first reported by Guan and Smart in 2000 in the CuCl/2,2′-bipyridine catalyzed polymerization of MMA using 2,2-dichloroacetophenone as an initiator under visible light irradiation [70]. They observed significant rate enhancement of the

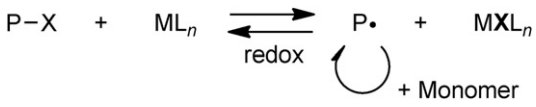

Scheme 5. Activation/deactivation mechanism in ATRP.

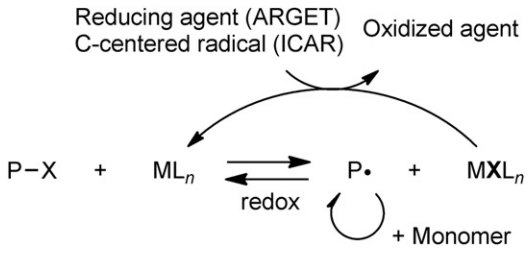

Scheme 6. Mechanism of ARGET and ICAR ATRP.

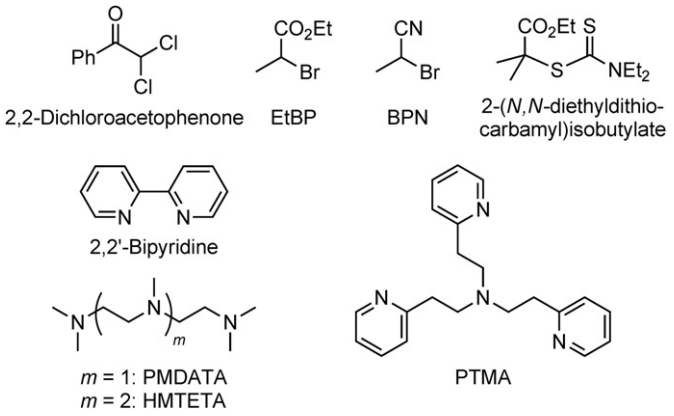

Chart 1. Initiators and ligands used for photo-ATRP.

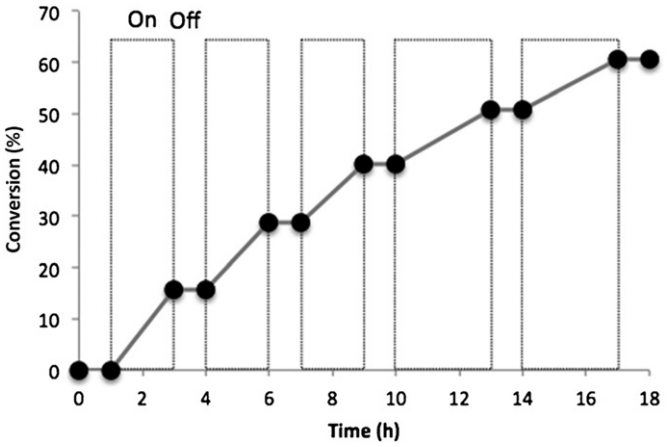

Fig. 1. Correlation between monomer conversion and time in the polymerization of MMA using *fac*-Ir(ppy)$_3$ as a catalyst while cycling the reaction's exposure to visible light. Reprinted with permission from Ref. [80]. Copyright 2012 John Wiley and Sons.

polymerization by employing 100 ppm of catalyst loading (~0.1 equiv of CuCl over the initiator). They also observed improved living character up until nearly quantitative monomer conversion. Though the effect of photoirradiation was not completely clear, they proposed that C–Cl bond homolysis in the inner sphere R–Cl/CuCl complex is enhanced by visible light irradiation. Note that a kinetic study of the same conditions by Kwak and Matyjaszewski suggested that photoirradiation has a negligible effect on the activation constant [71]. Further studies are needed to clarify this point.

Since Cu(II) species are photochemically reduced in the presence of amine ligands, Yagci and coworkers used this reaction to generate active Cu(I) species from air stable Cu(II) species [72]. The mechanism is similar to ARGET ATRP, though a stoichiometric or substoichiometric Cu(II) catalyst over an ATRP initiator was employed. For example, polymerization of MMA in the presence of ethyl bromopropionate (EtBP) as an initiator and $CuBr_2$/*N,N,N′,N″,N″*-pentamethyldiethylenetriamene (PMDATA) (Chart 1) under ~350 nm light irradiation followed the first-order kinetics after an induction period to reduce Cu(II) to Cu(I). The reaction gave well-controlled PMMA with M_n close to the theoretical value up to ~17,000 and a narrow MWD ($M_w/M_n < 1.3$). The rate of polymerization was much faster under this condition than that observed in the conventional Cu(I)-catalyzed ATRP. The fidelity of the polymer-end-functional group was ascertained by a chain extension experiment. The same group also reported that the addition of methanol enhanced the reactivity of the photo-induced ATRP [73]. Methanol plays dual roles as a reducing agent of Cu(II) to Cu(I) and enhances the solubility of Cu(II) species. Photoinitiators [74] or dyes [75] are also effective reducing agents of Cu(II) and facilitate the photo-induced ATRP of MMA. The amount of metal catalyst could be reduced to 0.1 equiv over the initiator under the dye-sensitized condition, but further reduction led to a loss of control. The polymerization of methyl acrylate (MA) and St was also examined under similar conditions, but the applicability was not confirmed, as the polymers formed had only low molecular weight or broad MWD.

Mosnáček and Ilčíková achieved a reduction in the amount of Cu catalyst in the photo-ATRP of MMA by using 2-bromopropionitrile (BPN) as an initiator [76]. When 100 ppm of $CuBr_2$/PMDATA catalyst (0.02 equiv over BPN) was used in 25 vol% of anisol as a solvent, controlled polymerization proceeded, giving PMMA having M_n close to the theoretical value (16,900 [exp] *vs.* 16,130 [theo]) and with narrow MWD ($M_w/M_n = 1.13$). The rate of polymerization as well as the level of control were very similar to ARGET ATRP using tin(II) octanoate as a reducing agent. The catalyst loading could be further reduced to 50 ppm by using tris(2-pyridylmethyl)amine (TPMA) as a ligand with maintaining a high level of control, but further reduction of the Cu catalyst loading to 25 ppm resulted in a loss of control. The higher efficiency of the TPMA ligand over PMDATA was attributed to the higher stability of the Cu(II) complex of the former ligand than that of the latter.

An alternative photo-ATRP approach is to utilize a photoredox catalyst [77,78] for the activation of dormant species. Park, Choi, and coworkers reported that Ru(byp)$_3$Cl$_2$ (bpy refers to 2,2′-bipyridyl) catalyst in the presence of tertiary amine effectively reduced ATRP initiators, such as BPN, under visible light irradiation and initiated polymerization of methacrylate derivatives [79]. Although polymerization was triggered by the photoirradiation, the system was not living, because the M_n values of the resulting polymer deviated considerably from the theoretical M_n, and the MWDs were also broad ($M_w/M_n > 1.7$).

Successful photoredox-catalyzed ATRP was reported recently by Fors and Hawker, who employed *fac*-Ir(ppy)$_3$ (Scheme 7a) as a catalyst in MMA polymerization using ethyl 2-bromo-2phenylacetate

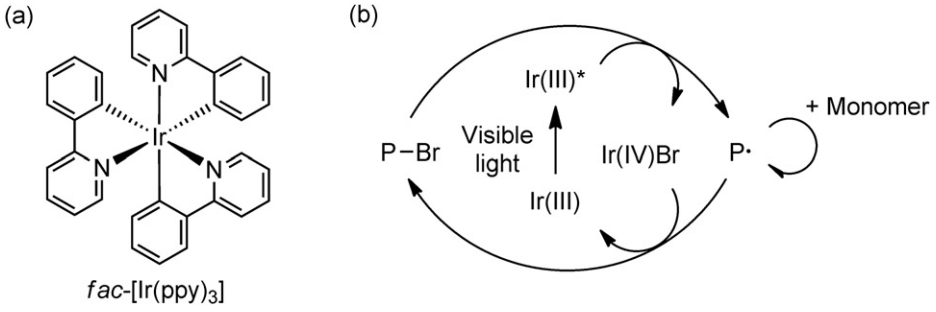

Scheme 7. (a) Structure of photoredox active Ir complex and (b) its mechanism of action under photochemical ATRP.

as an initiator under irradiation with a 50 W fluorescent lamp [80]. The amount of Ir catalyst played a key role in the control, and the use of 0.0125 equivalent of the catalyst over the initiator (~50 ppm level of the catalyst) gave structurally well-controlled PMMA with M_n close to the theoretical value from 2900 to 22,900 with a low MWD ($M_w/M_n < 1.25$). High catalyst loading, such as 0.5 equivalent over the initiator, resulted in uncontrolled PMMA. Polymerization proceeded only under photoirradiation, and polymerization ceased when the light was turned off. However, polymerization was restarted by photoirradiation, giving chain elongated PMMA even after turning the light on and off five times (Fig. 1). These results, combined with the linear growth of M_n along with conversion and the first-order kinetics to monomer, clearly reveal the living character. The polymerization proceeded with high end group fidelity, and PMMA having a bromine-end cap group was successfully used for the synthesis of block copolymers, such as poly[(MMA)-*block*-(benzoyl methacrylate)] and poly[(MMA)-*block*-(methacrylic acid)].

The role of the photoredox catalyst is as follows (Scheme 7b). It absorbs visible light to afford photoexcited *fac*-[Ir(ppy)$_3$]*, which reduces a dormant species to give the desired polymer-end radical and Ir(IV)—Br complex. The Ir(IV) complex then serves as a capping agent of the propagating radical to regenerate the initial Ir(III) complex in the ground state, as well as a dormant species with a Br-end group. They suspected that the high catalyst loading results in the formation of excessive radical species, leading to a shift of the dormant/radical equilibrium towards the radical side.

Another photo-ATRP approach is a combination of photoiniferter and ATRP. As already described, photiniferter polymerization cannot be well-controlled because of the inefficient chain transfer reaction of the dithiocarbamate group deactivating a polymer-end radical to a dormant species. However, the addition of a metal catalyst significantly improved control of the molecular weight and MWD.

Qin and coworkers reported that a binary photoinitiating system, 2,2-dimethoxy-2-phenylacetophenone (DMPA)/Fe[SC(S)NEt$_2$]$_3$, was successfully applied to the controlled polymerization of MMA [81]. The polymerization follows the typical living character, showing the linear evolution of M_n with monomer conversion, which follows the first-order kinetics, and the MWD was kept low (M_w/M_n ~1.5). Chain extension from the macro initiator was also successful. The initiation efficiency of DMPA was about 0.79 regardless of the concentration of Fe[SC(S)NEt$_2$]$_3$. M_n was independent of the concentration of the iron catalyst, whereas a high iron catalyst concentration led to a lower polymerization rate but higher MWD control. Although the mechanism was not fully clarified, the proposed initiation reaction involves photolysis of DMPA, generating benzoyl radical and α,α-dimethoxybenzyl radical, which further decompose to benzophenone and methyl radical (Scheme 8). Benzoyl and methyl radicals serve as initiating radicals ($R\cdot$) and react with Fe[SC(S)NEt$_2$]$_3$, generating an initiator, R—SC(S)NEt$_2$ and Fe[SC(S)NEt$_2$]$_2$. The initiating radical may also react first with monomer(s), followed by Fe[SC(S)NEt$_2$]$_3$, giving oligomeric dormant species P—SC(S)NEt$_2$ and Fe[SC(S)NEt$_2$]$_2$. The propagation step involves the activation of both R—SC(S)NEt$_2$ and P—SC(S)NEt$_2$ by Fe[SC(S)NEt$_2$]$_2$ under UV light irradiation, generating active radical species.

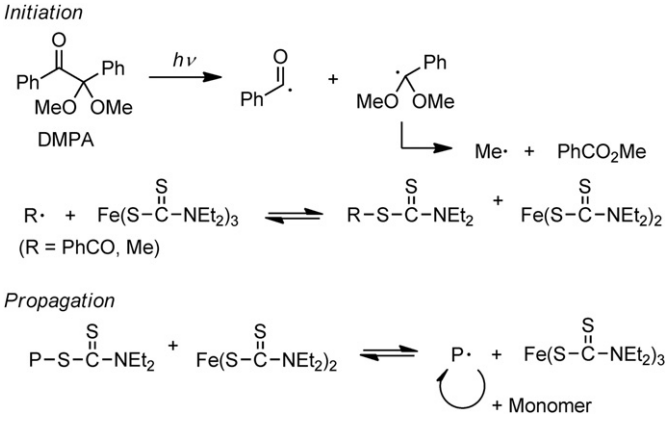

Scheme 8. Initiation and propagation mechanism of DMPA-initiated Fe-catalyzed photo-ATRP.

Kwak and Matyjaszewski reported the use of an isolated photoiniferter initiator, ethyl 2-(*N*,*N*-diethyldithiocarbamyl)isobutylate, and CuBr/*N*,*N*,*N*′,*N*″,*N*‴,*N*‴′-hexamethyltriethylenetetramine (HMTETA) for the controlled polymerization of MMA under UV irradiation (Chart 1) [71]. About 70-fold enhancement of the activation of the dormant species by the UV irradiation was observed, leading to good MWD control. PMMAs having M_n close to the theoretical value and with narrow MWD were obtained. The mechanism involves the photolysis of the dormant species, P—SC(S)NEt$_2$, generating P and SC(S)NEt$_2$ radicals (Scheme 9). The dithiocarbamyl radical was trapped by CuBr, generating CuBr[SC(S)NEt$_2$], which serves as an effective trapping agent of the polymer-end radical.

2.3. Photochemistry in CMRP

Porphyrin—Co complexes and Co(acac)$_2$ based organocobalt complexes have been used for CMRP [33,34]. Homolytic cleavage of the carbon—Co bond in the dormant species is the main activation mechanism [36]. CMRP is unique in polymerizing nonconjugated monomers such as vinyl acetate (VAc) and *N*-vinyl pyrrolidone (NVP) in a controlled manner. In particular, CMRP is the only method that can synthesize structurally controlled PVAc with high molecular weights (M_n ~ 100,000) while keeping a low MWD ($M_w/M_n < 1.4$) [34]. The dormant species derived from VAc is efficiently activated by thermolysis at ambient temperature generating the polymer-end radical and Co(II), which serves as a persistent radical, and these species are under active equilibrium. The carbon—Co bond in the dormant species derived from conjugated monomers, on the other hand, is so weak that the activation/deactivation equilibrium shifts to the radical side even at low temperature. Therefore, while acrylonitrile and acrylates were polymerized in a controlled manner under limited conditions, controlled polymerization of other conjugated monomers, such as St and methacrylates, has been difficult so far [82].

When Co(acac)$_2$ is used for the Co source, there are three methods to carry out CMRP. The first method involves a ternary system consisting of an azo-initiator, Co(acac)$_2$, and monomer at moderate temperature (~30 °C). The second method also involves a ternary system consisting of a peroxide as a redox initiator, Co(acac)$_2$, and monomer [83]. The third method utilizes a preformed alkyl-Co(acac)$_2$ complex formed by the reaction of the azo-initiator-derived radical and Co(acac)$_2$ [84]. When acrylates are used as monomers, only the second and third methods are efficient [85]. The first one leads to an exothermic reaction and an uncontrolled process, because the temperature needed to activate an azo-initiator also activates the Co—C bond in the dormant species.

Detrembleur and coworkers succeeded in the controlled polymerization of BA by generating a Co-initiator by the photolysis of

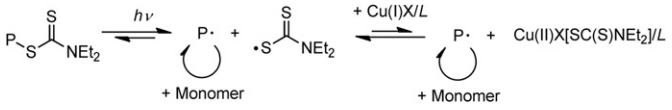

Scheme 9. Mechanism of photoiniferter-ATRP.

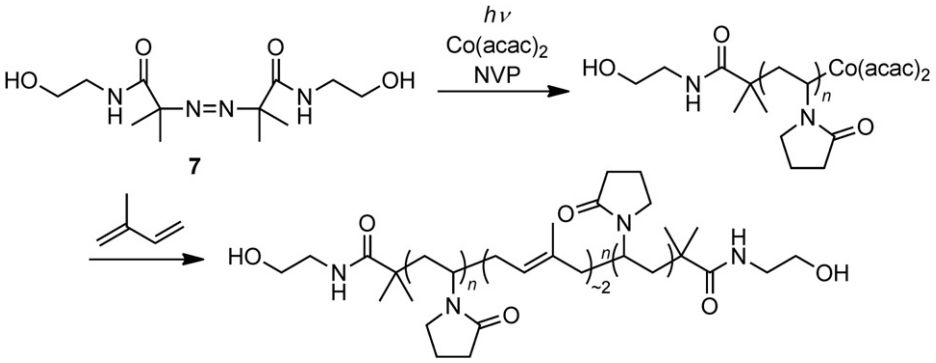

Scheme 10. Synthesis of hydroxyl-functionalized telechelic PNVP.

radical initiators at low temperature [86]. For example, AIBN was photolyzed in the presence of $Co(acac)_2$ at 0 °C, and subsequent polymerization of BA was carried out without photoirradiation at 30 °C. The resulting polymers were well-controlled with very high M_n (515,000–4,328,000) while keeping a low MWD (M_w/M_n = 1.33–1.38), though the initiation efficiency of AIBN was extremely low (<0.1%). A large amount of $Co(acac)_2$ remained in the reaction mixture, which caused the low polymerization rate. The initiation efficiency was improved to ~3% when DMPA was used as a photoinitiator. Structurally well-controlled PBAs having M_n from 6000 to 20,000 with low MWD (M_w/M_n ~ 1.24) were synthesized. Polymerization under UV irradiation was also examined, but the polymerization was not well-controlled, and tailing in the low molecular weight region was observed by gel permeation chromatography. Since organocobalt(III) compounds are photosensitive and generate carbon-centered radicals, the results must be due to the polymer-end radical coupling reaction as the photoirradiation generates excessive radical species from the dormant species (see Sections 2.7 and 3).

The same group also reported the synthesis of telechelic polymers starting from azo-initiator **7** having a hydroxyl functional group (Scheme 10) [87]. Thus, the photochemical reaction between **7** and $Co(acac)_2$ gave hydroxyl-functionalized organocobalt initiator, which was directly used for the polymerization of NVP. Subsequent isoprene-mediated polymer-end coupling afforded bis-hydroxyl-functionalized PNVP with narrow MWD.

2.4. Effect of α-polymer-end structure under DT mechanism

DT is the exclusive mechanism in RAFT [88] and the predominant one in TERP [89,90], IRP [91], SBRP [92], and BIRP [26]. The characteristic feature of the DT mechanism is that the activation and deactivation reactions are coupled with each other and controlled simultaneously. This is in sharp contrast to the RT mechanism, in which enhancement of the activation reaction sometimes results in a loss of control due to insufficient deactivation reactions [93,94]. A disadvantage of DT, however, is the need for influx of initiating radical species, usually from radical initiators, because the number of radical species does not change in DT. The addition of an initiator results in the formation of a polymer possessing an α-structure derived from the initiator, and complete control of the polymer is, in principle, unachievable, as schematically shown in Scheme 11. Furthermore, the influx of radical species increases the occurrence of the termination reaction, leading to dead polymers. The drawback of the radical initiator is more pronounced in block copolymer synthesis because a homopolymer of the second monomer forms from the initiator-derived radicals [95]. However, quantitative analysis of the effect of an azo-initiator on the α-polymer-end structure has not been clarified until recently.

Yamago and coworkers systematically analyzed the structural effect of azo-initiators on DT-mediated LRP. For example, polymerization using CTA **8** in the presence of AIBN gave polymers **9** and **10**, which possess α-end structures derived from the CTA and the azo-initiator, respectively (Scheme 12) [96]. The amounts of **9** and **10** were quantitatively determined by matrix-assisted laser desorption/ionization time-of-flight mass spectroscopy (MALDI-TOF MS) after reducing the polymer-end group to **11** and **12** (Fig. 2).

When St (30 equiv) was used as a monomer in the presence of 0.5 equivalent of AIBN and **8** (1 equiv) at 60 °C, AIBN-derived polymer **10** formed at about 4–7 % in all cases regardless of the CTA, such as X = TeMe (**8a**), $SbMe_2$ (**8b**), $BiMe_2$ (**8c**), I (**8d**), and SC(S)Ph (**8e**), which are used for TERP, SBRP, BIRP, IRP and RAFT, respectively. The formation of **10** increased with the increase of AIBN (Fig. 3). When 1 equivalent of AIBN was used, more than 10% of PSt possessed an α-polymer-end structure derived from the AIBN. Since 0.5–1 equivalent of AIBN was used in the polymerization of St, it was necessary to take care about the fidelity of the α-polymer-end structure.

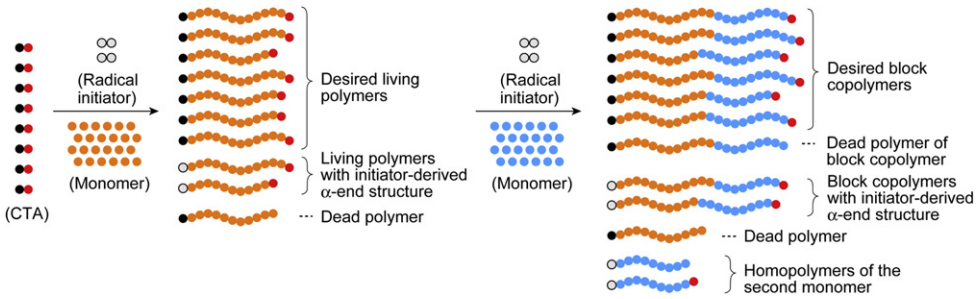

Scheme 11. Schematic representation of the effect of the radical initiator on polymer-end structures. Reprinted with permission from Ref. [96]. Copyright 2011 American Chemical Society.

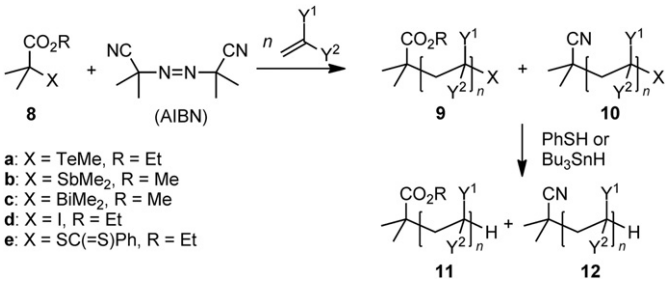

Scheme 12. Effect of AIBN on the structure of α-polymer-end.

Polymerization of isoprene (Ip) at 100 °C under the TERP conditions using **8a** and V-30 (0.5–1.0 equiv) also gave 5–10% of **10**. On the contrary, formation of **10** was negligible (<0.7%) in the polymerization of MMA, BA, and NBP when 0.5 equiv of AIBN was employed.

Polymer **10** forms via two pathways (Scheme 13). One pathway (path A) involves a direct chain transfer reaction of AIBN-derived radical with either CTA or a dormant species, giving cyano-substituted CTA **13**. Since **13** is an excellent CTA [16,24,26,89], it undergoes DT-mediated polymerization to give **10**. The other pathway (path B) proceeds via initial addition of the AIBN-derived radical to the monomer to give an oligomer radical, which undergoes chain transfer with either the CTA or a dormant species

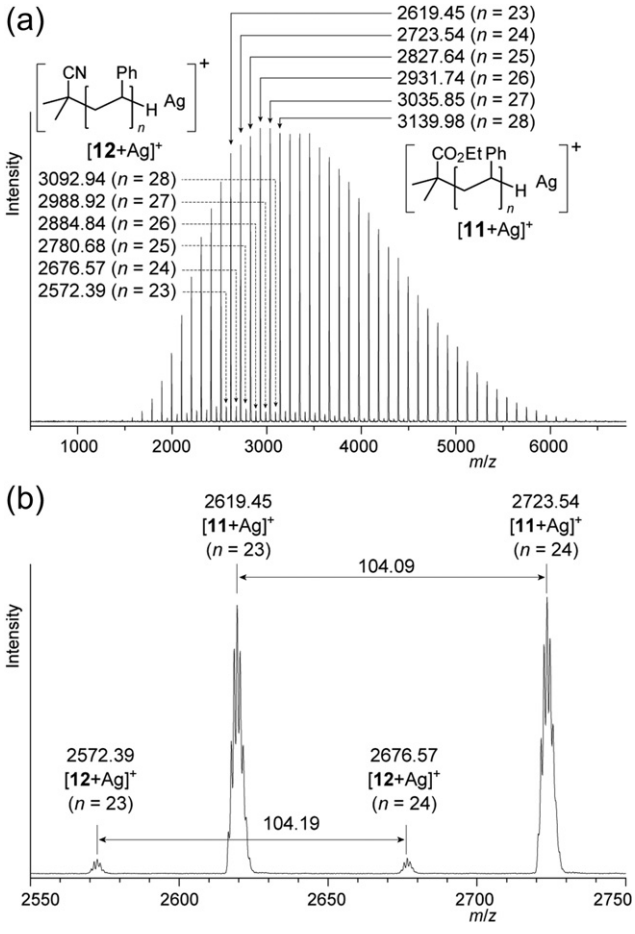

Fig. 2. (a) Full and (b) partial MALDI-TOF MS spectra of PSt obtained from polymerization of St (30 equiv) in the presence of **8a** and AIBN (0.3 equiv). The peaks correspond to the silver ion adduct $[M + Ag]^+$.

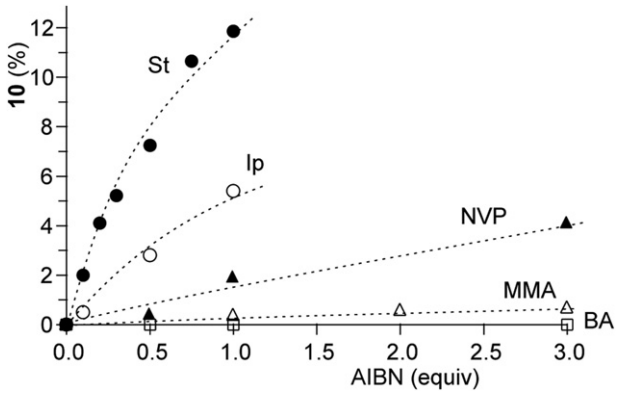

Fig. 3. Effect of AIBN on the structure of α-polymer-end. The ratio of **10** (%) versus the amount of AIBN (equiv) from the polymerizations of St (filled circles), isoprene (Ip, open circles), NVP (filled triangles), MMA (open triangles), and BA (open squares). V-30 instead of AIBN was used for the polymerization of Ip.

to give an oligomeric dormant species. Subsequent DT-mediated polymerization affords **10**. The mechanism indicates that the amount of the azo-derived radicals generated during the polymerization determines the amount of **10**, when chain transfer between the radical species and CTA or dormant species is efficient. Therefore, the amount of **10** increased with an increase in the amount of AIBN. In addition, since polymerization of monomers having low propagation rate constant require longer reaction time than those having high rate constant, the amount of **10** also increased for such monomers. The amount of **10** would also increase when the targeted M_n increase. Therefore, while the amount of **10** depend on the monomer species and is negligible for monomers having high propagation constants, the complete control of α-polymer-end structure is impossible by the addition of radical initiator under the DT-mediated polymerization.

One way to reduce the amount of **10** is to carry out the polymerization at high temperature by using an azo-initiator which decomposes at high temperature. An alternative and more promising way is to use photochemical activation of the dormant species, which generates initiating radicals. The following sections mainly deal with such chemistry.

2.5. Photo-induced RAFT

RAFT proceeds exclusively by the DT mechanism, in which polymer-end radical *P* reacts with dormant species P′SC(=S)Z, giving a new polymer-end radical *P*′ and dormant species PSC(=S)Z. DT proceeds in a stepwise manner through dithioacetal radical intermediate **14** (Scheme 14). The lifetime of **14** should be short in order to minimize unwanted radical–radical termination processes

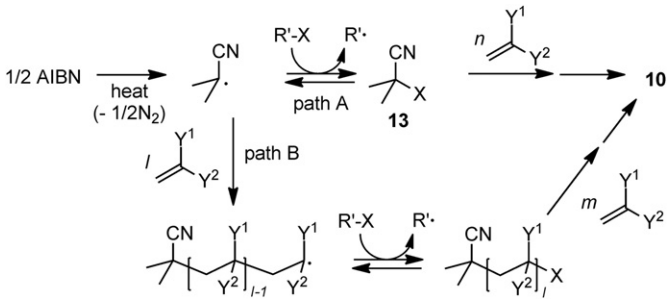

Scheme 13. Mechanism of the formation of AIBN-radical derived polymer **10.**

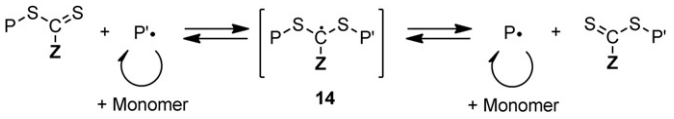

Scheme 14. Activation/deactivation mechanism of RAFT.

that would kill the chain reaction [97–99]. Both conjugated and nonconjugated monomers are polymerized in a controlled manner by an appropriate choice of *Z* group. Also, thiocarbonyl CTAs are compatible with a variety of functional groups and conditions, such as weak basic and acidic conditions. Furthermore, polymerization proceeds under mild conditions by an adequate choice of the azo-initiator. Due to this versatility, RAFT has been widely used for the synthesis of functional polymer materials.

RAFT under ^{60}Co γ-ray radiation has been reported to realize polymerization under mild thermal conditions. In 2001, Pan, Bai, and coworkers reported that γ-ray radiation initiated the controlled polymerization of MA, MMA, and St in the presence of dibenzyl trithiocarbonate (DBTTC) (Chart 2) [100]. When MA was polymerized under γ-irradiation in the absence of DBTTC, cross-linked PMA formed. However, the same polymerization in the presence of DBTTC afforded structurally controlled linear PMA with M_n close to the theoretical value ranging from 3,600 to 29,480 and low MWD (M_w/M_n = 1.08–1.15). MMA and St were also polymerized in a controlled manner. Davis and coworkers also reported the effectiveness of γ-irradiation on RAFT polymerization of St, including graft polymerization from PSt using 1-phenylethyl phenyldithioacetate (1-PEPDTA) as a CTA [101]. While detailed data were not described, PSts showing unimodal GPC traces were formed.

UV–vis light, which are far more readily accessible than γ-radiation, have also been used to carry out RAFT polymerization in the absence or in the presence of a photoinitiator. In 2002, Pan and coworkers reported the first example of RAFT by UV irradiation: polymerization of St and acrylates proceeded under irradiation with a broadband Hg lamp (8 W) in the presence of dibenzyl trithiocarbonate as a CTA [102]. Polymerization showed typical living character, such as first-order kinetics on monomer concentration, linear growth of M_n on monomer conversion, predictable M_n from the theoretical value, and narrow MWD. The resulting polymer was successfully used for the synthesis of block copolymers, revealing the high end group fidelity. Rizzardo, Davis, and coworkers also reported RAFT of St and MMA under UV irradiation (λ_{max} = 365 nm, 60 μW cm^{-2}) using 1-phenylethyl phenyldithioacetate (1-PEPDTA) or 1-phenylethyl dithiobenzoate (1-PEDB) as a CTA [103]. The polymerization showed living character at low monomer conversion (up to 30%), giving well-controlled polymer with a narrow MWD, but loss of the living chain-end and broadening of the MWD were observed at high monomer conversion. The discrepancy between these two results on the livingness probably originates from the intensity of the light source. A higher intensity of the light source leads to the generation of more radicals from the dormant species, which leads to an increase of dead polymers.

Sunlight- [104] and plasma-initiated [105] RAFT, in combination with conventional RAFT CTAs, were also reported. A new photo-iniferter/RAFT agent, phenyacyl morpholine-4-dithiocarbamate (PMDC), was also developed by Yagci and coworkers and was used for St polymerization under UV irradiation [106].

The mechanism of RAFT under γ and UV–vis irradiation is essentially identical to that under thermal conditions, as shown in Scheme 14 [107,108]. The difference is the source of the initiating radical species, which are not completely characterized under γ-ray radiation. The contribution of direct radiolysis of RAFT agents was clarified by identification of the dithioacetate-initiated polymer via mass spectrometry by Stenzel, Barner-Kowollik, and coworkers [109], and monomers and water in the reaction media also generated initiating radicals upon γ-ray irradiation.

Photolysis of RAFT CTAs occurs under UV irradiation, which provides an initiating radical. Cai and coworkers reported that short-wavelength UV had a detrimental effect on the RAFT agent, and that controlled polymerization occurred by irradiation of long-wavelength UV (λ > 365 nm) in the presence of a photoinitiator [110,111]. All of these results suggest that not only the intensity but also the wavelength of the light must be carefully selected to maintain high end group fidelity throughout the polymerization. Once an initiating radical is provided by any means, the polymerization proceeds by the DT mechanism. These results suggest that complete control of the α-end structure would be possible only under direct photolysis of the RAFT agent.

Because of the mechanistic similarity of RAFT under γ-, UV-, and sunlight-irradiation with that under thermal conditions, the choice of the *Z* group of CTA under irradiation follows that under thermal conditions. Several RAFT CTAs, such as dithiocarbamate (Z = NR_2) [112], xanthate (Z = OR) [113], and dithioesters (X = R) [114] including *in situ* generated dithioester from dithiobenzoic acid [115], were successfully used. Since the characteristic features of RAFT, such as the high monomer versatility and functional group compatibility, are preserved, monomers having polar functional groups, such as acrylic acid [116,117] and *N*-isopropyl acrylamide (NIPAM), were successfully polymerized in a controlled manner [118]. Polymerization of NIPAM in water could be carried out at a temperature of around 20 °C, which is much lower than the lower critical solution temperature of PNIPAM in water. An alternating copolymer, poly[St-*alt*-(malenic anhydride)] [119], random copolymers, such as poly(St-*co*-MA) and poly(St-*co*-BA) [108], and ABA-symmetrical triblock copolymers consisting of St and MMA from DBTTC were also prepared [120].

2.6. Photo-induced IRP

IRP, developed by Tatemoto and coworkers, is one of the oldest LRP methods [40]. The method is particularly suitable for the controlled polymerization of fluorinated monomers and has been used already in industry for producing fluorinated polymer materials [41]. The drawback, however, is its low applicability to conventional monomers, and polymers with a broad MWD (M_w/M_n > 1.5) are usually obtained [11,121]. IRP predominantly proceeds by the DT mechanism and is usually carried out by the addition of a radical initiator because the contribution of RT is small.

A dinuclear manganese carbonyl complex, $Mn_2(CO)_{10}$, undergoes photochemical homolysis of the Mn–Mn bond under visible light irradiation to form the highly reactive metal-centered radical •$Mn(CO)_5$ [122]. It abstracts halides from a variety of organohalogen compounds, generating the corresponding carbon-centered radicals (Scheme 15). Kamigaito and coworkers were the

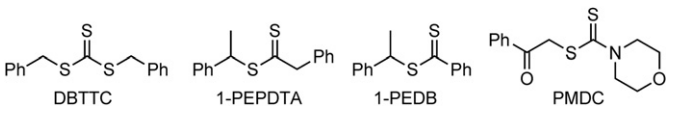

Chart 2. CTA used for photo-RAFT.

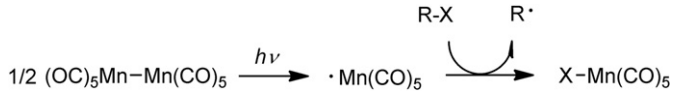

Scheme 15. Generation and reaction of manganese radical under photoirradiation.

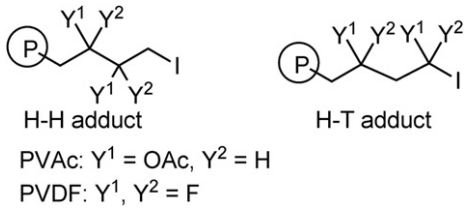

Chart 3. Dormant species derived from the head-to-head and head-to-tail addition.

first to utilize $Mn_2(CO)_{10}$ as a photoactivator of organoiodine dormant species under visible light irradiation [123]. Since the reverse reaction between *R* radical and *X*–$Mn(CO)_5$ regenerating *R*–*X* and •$Mn(CO)_5$ is less likely due to the strength of the I–Mn bond [124], the contribution of the RT mechanism must be quite limited.

Polymerization of VAc with ethyl iodoacetate as a CTA in the presence of $Mn_2(CO)_{10}$ and tributylamine under 27 W fluorescent light irradiation reached more than 90% monomer conversion in a few hours at 40 °C. Polymerization also proceeded in the absence of tributylamine and gave controlled polymers, but the addition of the amine increased the polymerization rate. The concentration of $Mn_2(CO)_{10}$ had almost no effect on M_n, and the use of 0.025–0.25 mol % relative to the monomer was sufficient to promote polymerization. The polymerization showed a living character in that M_n increased linearly with respect to the monomer feed, which can be predicted from the monomer/CTA ratio. The MWDs were unimodal and relatively narrow ($M_w/M_n \sim 1.2$) in the early stages of the reactions ($M_n < 10{,}000$), but the MWD control eroded as the conversion increased. PVAc with $M_n \sim 19{,}000$ was prepared, but M_w/M_n increased to ~1.8. Photoirradiation was essential for polymerization to proceed, and monomer feed ceased immediately upon turning off the light source. However, the reaction proceeded again when the light was turned on and finally resulted in almost quantitative monomer conversion. PVAcs with almost the same M_n and MWD as those with continuous light irradiation were obtained.

The loss of MWD control at high monomer conversion is due to the accumulation of unreactive dormant species formed by the head-to-head addition [H–H adduct (Y^1 = OAc, Y^2 = H) in Chart 3] [90,125,126]. The H–H adduct possesses a C–I terminal that is far less reactive toward the regeneration of polymer-end radicals than the head-to-tail adduct (H–T adduct) is. The amount of H–H adduct was 14% at 21% monomer conversion and increased to 73% at 96% monomer conversion. Although the activation of the H–H adduct in regenerating the polymer-end radical was not clarified, it should occur considering the high reactivity of the manganese radical (see below), and this reactivation contributed considerably to the observed good MWD control.

$Mn_2(CO)_{10}$ also induced IRC of conjugated monomers, such as MA and St [123]. Good MWD control was observed for St polymerization by using ethyl 2-iodobutylate as a CTA when the targeted M_n was low (~15,000), but polymerization of MA was not well-controlled, probably due to the inefficient DT reaction. Kamigaito and coworkers also employed the photoactivation of $Mn_2(CO)_{10}$ in the copolymerization of MA and VAc [127] and the copolymerization of MA and 1-hexene [128]. Although unimodal copolymers were obtained, control of the MWD was limited ($M_w/M_n > 1.5$). The manganese system is compatible with protic solvents, and the copolymerization of MA and 1-hexene in fluoroalcohols, such as $(CF_3)_2CHOH$ and $(CF_3)_3COH$, afforded a resulting copolymer with a high 1-hexene fraction. An alternating copolymer from MA and 1-hexene formed by the use of excess 1-hexene over MA in fluoroalcohol, though control of the MWD was low ($M_n \sim 6000$, $M_w/M_n \sim 1.8$). Fluoroalcohols act as Brønsted acids and coordinate to the ester of MA and MA-derived radical, enhancing the electrophilicity of MA and the radical. Since α-olefin is a necleophilic acceptor, the more electrophilic it is, the more the acid-coordinated radical increases the cross propagation to 1-hexene.

Asandei and coworkers utilized $Mn_2(CO)_{10}$ photoactivation in the polymerization of fluorinated monomers under mild thermal conditions at low pressure, in contrast to the conventional polymerization of fluorinated monomers, which requires high temperature and high pressure [129]. A variety of organohalides were effective in inducing polymerization of vinylidene fluoride (VDF) in the presence of $Mn_2(CO)_{10}$ under weak fluorescent lamp irradiation, but mono and bifunctional perfluorinated alkyliodides, such as $F(CF_2)_nI$ (n = 1–4) and $I(CF_2)_6I$, were preferred CTAs. The reactions gave PVDFs with M_n ranging from 1,000 to 23,000 with good to moderate MWD control (M_w/M_n = 1.2–1.7). This initiating system is also effective for polymerization of CF_2=CFCl, CF_2=CCl_2, CF_2=CFBr, CH_2=CFG, and VDF random copolymers with CF_2=$CF(CF_3)$ and CF_2=$CF(OCF_3)$.

Polymerization of VDF also generated the H–H adduct in addition to the H–T adduct (Chart 3, Y^1, Y^2 = *F*), and the accumulation of the H–H adduct with monomer conversion contributed to the wider MWD. However, activation of the H–H adduct was suggested during the screening of organoiodine CTAs; primary alkyliodides and an H–H adduct model, $CF_3CF_2CH_2I$, initiated the polymerization of VDF in the presence of $Mn_2(CO)_{10}$ under photoirradiation. This reactivation of the H–H adduct helps to reduce the loss of MWD control at high monomer conversion.

Despite the formation of the H–H adduct, the total iodine functionality at the ω-polymer-end for both the H–H and H–T adduct was highly preserved (>95%). Therefore, PVDF–I and I–PVDF–I were used as macro CTAs for the synthesis of block copolymers. Structurally well-defined AB-diblock and ABA-triblock copolymers with St, vinyl chloride, VAc, MA, and acrylonitrile were successfully synthesized for the first time under $Mn_2(CO)_{10}$ activation conditions.

2.7. Photo-induced TERP

TERP proceeds predominantly by the DT mechanism, and the RT mechanism is involved in the polymerization at high temperature (~100 °C) [20,21]. Once the initiating radical is provided from organotellurium dormant species by the RT mechanism, it predominantly undergoes DT-mediated polymerization (Scheme 16). Therefore, no radical initiator is necessary under such conditions. However, the applicability is limited as only dormant

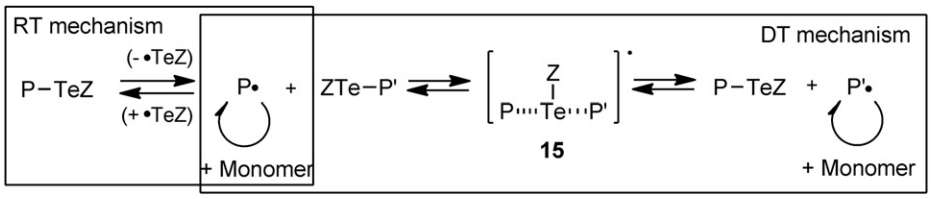

Scheme 16. Mechanism of TERP.

species having a weak C–Te bond, such as PSt and polymethacrylate, are effectively activated under these conditions. TERP proceeds under mild thermal conditions by the addition of an azo-initiator [89], and this condition is sufficient in many instances, including industrial-scale synthesis of functional polymers [130].

TERP is a highly synthetically versatile method. The most significant feature is high monomer versatility [21,89,131–136]; both conjugated and nonconjugated monomers are successfully polymerized in a controlled manner by using the same organotellurium CTA. The situation is in sharp contrast to RAFT, in which the substituent *Z* must be carefully selected depending on the monomer family (see Section 2.5). This is due to microscopic differences in the DT mechanism between RAFT and TERP [30,90]; RAFT proceeds via stable radical intermediate **14**, whereas no such stable intermediate is involved in TERP. Since the stability of **14** is insensitive to the monomer families but sensitive to the *Z* group, the *Z* group has to be carefully selected to realize an effective DT reaction. On the contrary, DT of TERP proceeds through a T-shaped transition state or short-lived intermediate **15**, the stability of which is highly sensitive to the monomer families and positively changes, achieving an effective DT reaction [90]. Furthermore, TERP is highly compatible with various polar functional groups and conditions, and many methods for the transformation of polymer-end groups for the synthesis of block copolymers [21,137–139] and end-functionalized polymers [20,140–143] have been developed. Therefore, TERP has been gaining much attention as the new method of choice to conduct LRP.

Yamago and coworkers reported TERP under weak-intensity photoirradiation in 2009 [131]. Organotellurium CTA, such as **16**, possesses UV–vis absorption corresponding to the n(Te)-σ^*(C–Te) transition at λ_{max} ~350 nm (ε = 260 mol L^{-1} cm^{-1}), and excitation of this transition induces C–Te bond homolysis. However, when the polymerization of BA was carried out in the presence of **16** in a Pyrex vessel under 500 W Hg lamp radiation, uncontrolled PBA with a high MWD was formed (M_w/M_n = 1.87). Formation of diphenyl ditelluride and deposition of Te metal was also observed in the reaction mixture, indicating loss of the phenyltellanyl polymer-end group. In contrast, when the reaction was irradiated through a short-wavelength cutoff filter (>470 nm) or 1% neutral density filter, PBAs with controlled M_n values formed within 2 h at ~50 °C. PBAs with M_n ranging from 13,000 to 223,000 and narrow MWDs (M_w/M_n = 1.09–1.18) were formed by changing the BA/**16** ratio. These conditions are in sharp contrast to those for TERP of BA under thermal conditions, which required 100 °C for 24 h to reach 89% monomer conversion.

Polymerization proceeded only under photoirradiation and stopped when the light was turned off. However, the polymerization restarted upon turning on the light again, and a chain extended polymer formed, while maintaining unimodality and a narrow MWD (Fig. 4). Well-controlled PBA with M_n of 12,400 and a narrow MWD (M_w/M_n = 1.10) was eventually obtained in 96% monomer conversion after three cycles of turning the light off and on. The results clearly showed that the tellurium ω-end group was preserved during the polymerization as the living end and that the amount of dead polymers was negligible. All of these results are consistent with the living character of photo-TERP.

Organotellurium compounds are highly photosensitive (Scheme 17). When CTA **16** and TEMPO were photolyzed under conditions identical to those in the photo-TERP described above, **16** completely disappeared within 10 min, and TEMPO adduct **17** and ethyl methacrylate were formed in quantitative combined yields. The phenyltellanyl group was quantitatively recovered as diphenyl ditelluride. Formation of **16** and ethyl methacrylate is from the direct coupling and β-hydrogen abstraction reactions between the radical generated from **16** and TEMPO, respectively. The same reaction in the dark required 100 °C for 94 h for the complete disappearance of **16**. The results clearly reveal the effectiveness of photoirradiation in generating carbon-centered radicals from organotellurium compounds.

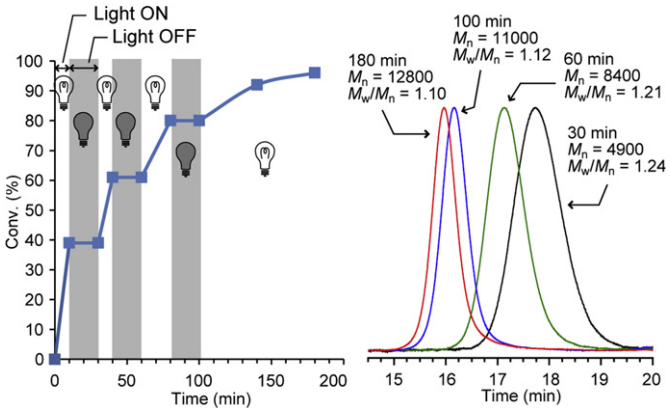

Fig. 4. Effect of photoirradiation on the progress of polymerization.

Weak-intensity light sources, such as 30–100 W black lamp, 6 W light emitting diode lamp, and even sunlight, are effective to activate the dormant species. The easy availability of the light source and the low energy cost make this feature attractive in practice. High-intensity light, on the other hand, generates excessive polymer-end radicals and increases the formation of dead polymers, but a high concentration of radical species can be successfully applied to the radical coupling reaction (See Section 3).

The high synthetic versatility of TERP is preserved under photo-TERP, and varieties monomers were polymerized in a controlled manner under photoirradiation (Fig. 5). Acrylates, acrylamides, acrylonitrile, methacrylates, St, and nonconjugated monomers, such as NVP, *N*-vinylimidazole, and *N*-vinylcarbazole, were successfully polymerized by using **8a** or **16** as a CTA. Monomer conversion reached nearly quantitative, and well-controlled polymers with narrow MWDs were obtained in all cases. The polymerization was compatible with polar functional groups, such as ethers, free hydroxyl group, carboxlic acid, and amide proton. Since activation of the dormant species did not require thermal stimulus, the polymerization could be carried out at low temperature, such as room temperature, and even below 0 °C. Therefore, isocyanate, which is a thermally unstable functional group, was also tolerable, and the TERP of isocyanide-tethered acrylate gave the desired polymer in a controlled manner. The polymerization at low temperature was also advantageous in reducing the formation of

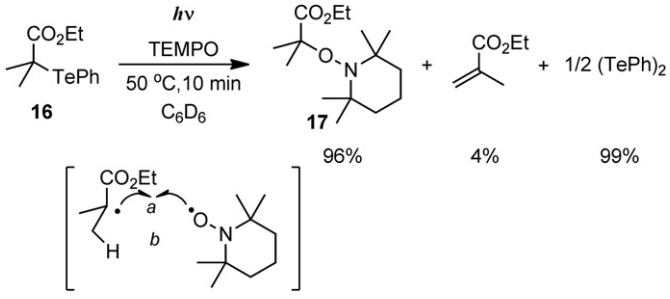

Scheme 17. Photo-induced reaction of **16** with TEMPO.

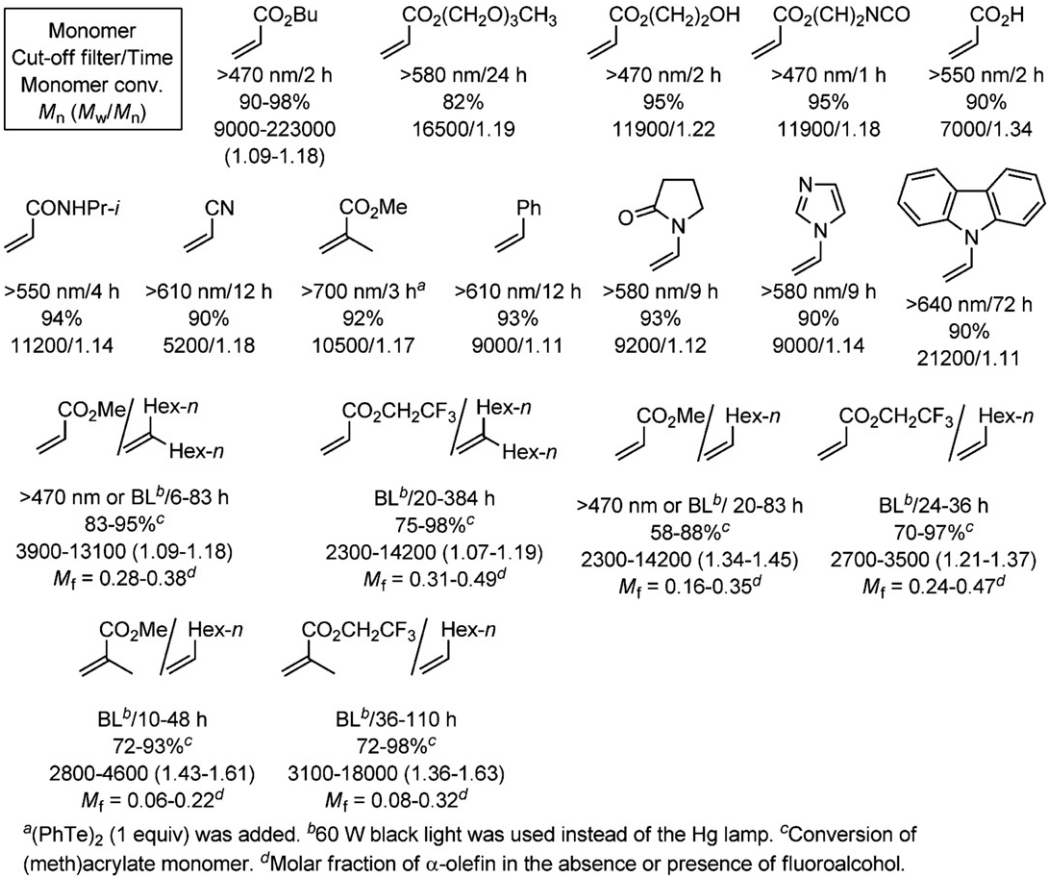

Fig. 5. Monomers polymerized by photo-TERP using **8a** or **16** as a CTA. Unless otherwise noted, photoirradiation was carried out with a 500 W Hg lamp through a short-wavelength cutoff filter.

branches caused by the back-biting reaction in acrylate polymerization [144]; whereas PBA (M_n = 50,000, M_w/M_n = 1.31) prepared in the dark at 100 °C had 2.1% branches, PBA (M_n = 54,000, M_w/M_n = 1.16) prepared under photoirradiation at 0 °C had almost no branches (<0.1%).

Photo-TERP was also applicable for the controlled copolymerization of (meth)acrylates and α-olefins (Fig. 5) [133]. When 6-methyleneundecane (6MU) as an α-olefin and MA or trifluoroethyl acrylate (TFEA) as an acrylate monomer were used, both photochemical and thermal conditions gave controlled copolymers having narrow MWDs. The addition of fluoroalcohol, such as 1,3-$C_6H_4[C(CF_3)_2OH]_2$ and hexafluoroisopropanol, as a Brønsted acid (see Section 2.6) and the use of an excess amount of 6MU over TFEA increased the molar fraction (M_f) of 6MU in the copolymers. When electrophilic TFEA was used as an acrylate, nearly alternating copolymer (M_f = 0.49) with controlled M_n = 5,900 and a narrow MWD (M_w/M_n = 1.19) was obtained.

When 1-octene was used as an α-olefin, copolymerization with (meth)acrylates under thermal conditions gave copolymers with considerably broad MWDs (M_w/M_n > 1.45). On the contrary, copolymerization under photoirradiation greatly increased the MWD control [136]. Structurally well-controlled copolymers with M_n values ranging from 3,000 to 18,000 and low MWDs (M_w/M_n = 1.22–1.45) were obtained. While a dormant species having a 1-octene unit at the polymer-end is more difficult to reactivate than that having acrylate and 6MU are, photoirradiation probably enhanced the activation of the inert dormant species (Chart 4). Addition of fluoroalcohol also increased the insertion of 1-octene into the copolymer. Nearly alternating copolymer (M_f ~0.5) also formed when TFEA was employed as an acrylate monomer and an excess amount of 1-octene over TFEA was used in the presence of fluoroalcohol.

The copolymer was used as a macro CTA for the synthesis of well-controlled block copolymers, suggesting that the tellurium group at the polymer-end was highly preserved. Poly[(TFEA-*co*-6MU)-*block*-St], poly[(MA-*co*-6MU)-*block*-St], poly[(MA-*co*-6MU)-*block*-NVP], and poly[(TFEA-*co*-1-octene)-*block*-TFEA] with narrow MWDs (M_w/M_n = 1.13–1.41) were synthesized. This is the first example of the use of this type of copolymer as a macro CTA in the controlled synthesis of block copolymers. The ω-polymer-end unit in the macroinitiators was mainly from 6MU and 1-octene, as analyzed by deuterium labeling experiments. While such polymer-end groups derived from α-olefins are less reactive and more difficult to reactivate than those from acrylates, the above experiments clearly revealed that both polymer-end groups were successfully activated.

The mechanism of photo-TERP is essentially the same as that under thermal conditions shown in Scheme 16. Once an organotellurium dormant species was activated by photolysis, the resulting

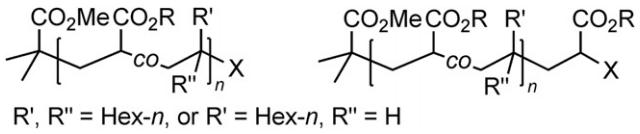

Chart 4. End group structures observed in the copolymerization of acrylate and α-olefin.

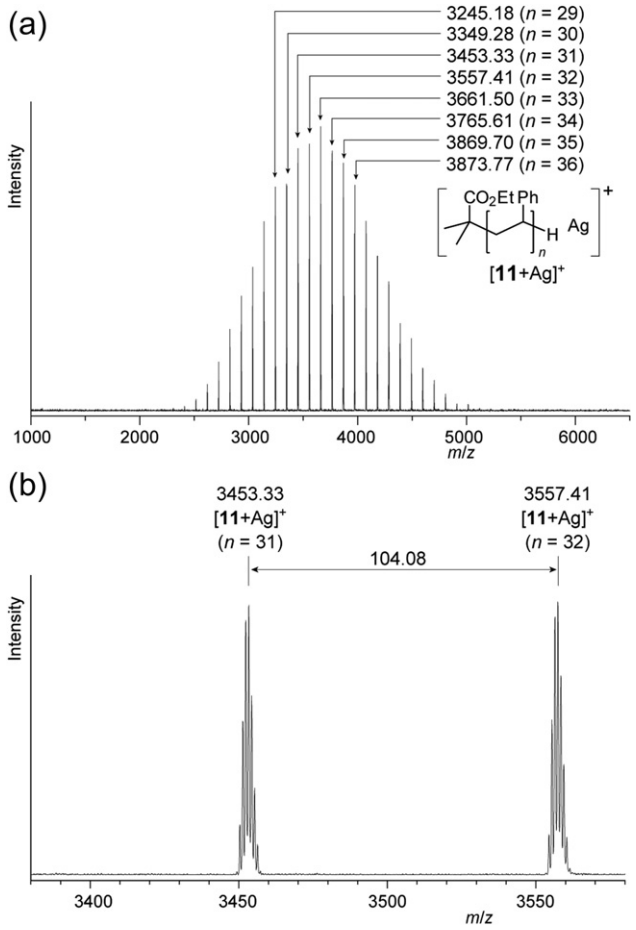

Fig. 6. (a) Full and (b) partial MALDI-TOF MS spectra of PSt obtained from polymerization of St (30 equiv) in the presence of **8a** under photo irradiation. The peaks correspond to the silver ion adduct $[M + Ag]^+$.

radical predominantly underwent DT-mediated polymerization. Since no radical initiator was necessary, the α-polymer-end structure was strictly controlled and preserved, as evidence by MALDI-TOF MS analysis (see Fig. 6, and also Fig. 2) [96].

Photoirradiation was also effective for the selective synthesis of block copolymers [96]. When St was polymerized in the presence of PMMA–TeMe macro initiator in the presence of 0.5 equiv of AIBN, 11% of PSt homopolymer formed in addition to the desired PMMA–PSt block copolymer. However, the same block copolymer synthesis under photoirradiation without AIBN exclusively gave PMMA–PSt block copolymer. All of these results clearly reveal the advantage of photochemical conditions in controlling the chain-end structure and in the selective synthesis of block copolymers.

3. Photo-induced transformation of polymers prepared by TERP

The efficient photochemincal activation of organotellurium dormant species was applied to the selective transformation of the ω-polymer-end via polymer-end radicals. For example, when PMMA **18a** prepared by TERP was photoirradiated in the presence of TEMPO using a 500 W Hg lamp though a 470 nm short-wavelength cutoff filter at 50 °C, ω-vinylidene PMMA **19a** formed quantitatively after 3 h. The structure of the starting polymer besides the ω-end was completely preserved in the product, as judged by ^{1}H NMR, MALDI-TOF MS, and GPC analyses (Scheme 18)

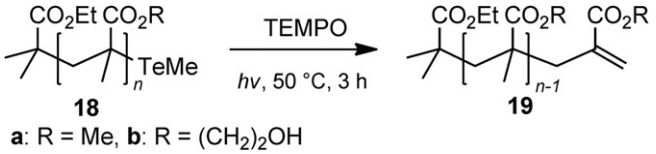

Scheme 18. Synthesis of ω-vinylidene functionalized polymethacrylates.

[142]. The same transformation at 100 °C in the dark required 24 h for completion, revealing the highly efficient generation of polymer-end radicals under photoirradiation. Poly(hydroxyethyl methacrylate) **18b** also transformed to **19b** in quantitative yield upon treatment with TEMPO under photoirradiation. The products would be useful as macromonomers and CTAs.

The mechanism of this transformation is identical to the one shown in Scheme 16. TEMPO irreversibly abstracts β-hydrogen of the polymethacrylate radical generated from **18**. The radical may also couple with TEMPO, giving a ω-TEMPO capped polymethacrylate. However, it regenerates the polymer-end radical under mild thermal conditions, and the irreversible reaction shifts the equilibrium and leads to the exclusive formation of **19**.

The difference of efficiency in generating radical species was applied to the photo-induced selective switching of the reaction course from radical polymerization to the radical coupling reaction (Scheme 19) [145]. It has been reported that the reaction course can be changed from LRP to the radical coupling reaction by adding an excess amount of Cu(0) to end-brominated polymer prepared via Cu(I) catalyzed ATRP [146–148] and by adding dienes to polymers prepared by CMRP, as shown in Scheme 10 [85,149–151]. However, this is the first report on the selective switching of the reaction course without chemical stimuli.

TERP of Ip was best controlled under thermal conditions by heating at 120 °C, and controlled PIp with M_n ranging from 3,500 to 19,900 and narrow MWDs (M_w/M_n = 1.09–1.15) formed. The addition of an azo-initiator resulted in loss of control due to the increased dead polymer formation, because the propagation rate constant of Ip is small (see Section 2–4). Once PIp formed, irradiation by a 500 W Hg lamp through a 390 nm short-wavelength cutoff filter selectively transformed the living polymer to the dimer with excellent coupling efficiency (X_c = 0.87–0.97). M_n of the coupling product was nearly double that of the precursor, and the MWD was kept narrow (M_w/M_n = 1.10–1.13). Starting from hydroxyl-functionalized CTA **20**, hydroxyl-telechelic PIp with controlled MWD was also prepared.

The dimer formed by a polymer-end coupling reaction, which is consistent with the termination mechanism of Ip polymerization under radical conditions. Because the coupling reaction under thermal conditions was sluggish and did not complete even after heating at 140 °C for 24, the high-efficiency generation of polymer-end radical by photolysis is responsible for the observed efficient coupling reaction.

This method can be readily applied to the synthesis of symmetric ABA-type block copolymers from organotellurium macro CTAs. For example, treatment of PSt–TeMe (M_n = 5,900, M_w/M_n = 1.15) with Ip at 120 °C gave a controlled diblock copolymer, poly(St-*block*-Ip)-TeMe (M_n = 9,700, M_w/M_n = 1.12), which, upon photoirradiation, was transformed to an ABA-triblock copolymer, poly(St-*block*-Ip-*block*-St) in a controlled manner (M_n = 17,000, M_w/M_n = 1.18) with high coupling efficiency (X_c = 0.86). Structurally well-controlled poly(MMA-*block*-Ip-*block*-MMA) (M_n = 12,800–28,900, M_w/M_n = 1.11–1.15) was also synthesized from PMMA-TeMe (M_n = 4,300–13,700, M_w/M_n = 1.16–1.18) by sequential thermal copolymerization of Ip and a photochemical radical coupling reaction.

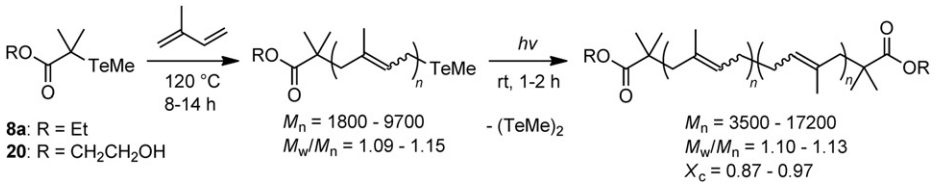

Scheme 19. Selective switching from TERP of Ip to polymer-end radical coupling. The main chain Plp consists of a mixture of three isomeric structures, and the major structure is shown here.

4. Summary

The use of photochemistry not only opens up new possibilities for overcoming the problems encountered in known LRP methods but also creates new opportunities for the use of LRP in macromolecular engineering for the synthesis of novel polymer materials. Activation of dormant species at low temperature in the RT mechanism is a direct and synthetically useful outcome of the use of photoirradiation. Activation of the dormant species having a strong C–X bond is particularly attractive and expands the synthetic scope of LRP involving nonconjugated monomers. Furthermore, the radical coupling reaction provides a novel synthetic route for symmetrical telechelic polymers and block copolymers. This type of reaction should also be applicable to the organic synthesis of small molecules. Since control of the radical concentration in the reaction mixture is the key in both LRP (low concentration) and the coupling reaction (high concentration), fine tuning of the radical generation by the irradiation intensity should lead to more-precise control in the synthesis of both macro- and small-molecules. Other attractive advantages are the reduction of metal catalyst loading in ATRP, and increased fidelity of the α-polymer-end structure in DT-mediated LRPs. Since these advantages of photoirradiation can be achieved with low-power, readily available light sources, the use of photo-LRP in industrial-scale synthesis should be feasible.

References

[1] Nesvadba P. In: Chatgilialoglu C, Studer A, editors. Encyclopedia of radicals in chemistry, biology and materials. Wiley; 2012. p. 1.
[2] Matyjaszewski K, Davis TP, editors. Handbook of radical polymerization. New York: Wiley-Interscience; 2002.
[3] Moad G, Solomon DH. The chemistry of radical polymerization. Amsterdam: Elsevier; 2006.
[4] Chain vinyl polymerization, vol. 3. Amsterdam: Elsevier BV; 2012.
[5] Cunningham MF. Prog Polym Sci 2008;33:365.
[6] Zetterlund PB, Kagawa Y, Okubo M. Chem Rev 2008;108:3747.
[7] Destarac M. Macromol React Eng 2010;4:165.
[8] Georges MK, Veregin RPN, Kazmaier PM, Hamer GK. Macromolecules 1993; 26:2987.
[9] Hawker CJ, Bosman AW, Harth E. Chem Rev 2001;101:3661.
[10] Kato M, Kamigaito M, Sawamoto M, Higashimura T. Macromolecules 1995; 28:1721.
[11] Gaynor S, Wnang J-S, Matyjaszewski K. Macromolecules 1995;28:8051.
[12] Matyjaszewski K, Xia J. Chem Rev 2001;101:2921.
[13] Kamigaito M, Ando T, Sawamoto M. Chem Rev 2001;101:3689.
[14] Braunecker WA, Matyjaszewski K. Prog Polym Sci 2007;32:93.
[15] Ouchi M, Terashima T, Sawamoto M. Chem Rev 2009;109:4963.
[16] Chiefari J, Chong YKB, Ercole F, Krstina J, Jeffery J, Le TPT, et al. Macromolecules 1998;31:5559.
[17] Lowe AB, McCormick CL. Prog Polym Sci 2007;32:283.
[18] Moad G, Rizzardo E, Thang SH. Polymer 2008;49:1079.
[19] Moad G, Rizzardo E, Thang SH. Acc Chem Res 2008;41:1133.
[20] Yamago S, Iida K, Yoshida J. J Am Chem Soc 2002;124:2874.
[21] Yamago S, Iida K, Yoshida J. J Am Chem Soc 2002;24:13666.
[22] Kayahara E, Yamago S, Kwak Y, Goto A, Fukuda T. Macromolecules 2008;41:527.
[23] Yamago S, Ray B, Iida K, Yoshida J, Tada T, Yoshizawa K, et al. J Am Chem Soc 2004;126:13908.
[24] Ray B, Kotani M, Yamago S. Macromolecules 2006;39:5259.
[25] Yamago S, Yamada T, Togai M, Ukai Y, Kayahara E, Pan N. Chem Eur J 2009; 15:1018.
[26] Yamago S, Kayahara E, Kotani M, Ray B, Kwak Y, Goto A, et al. Angew Chem Int Ed 2007;46:1304.
[27] Kayahara E, Yamago S. J Am Chem Soc 2009;131:2508.
[28] Yamago S. Proc Jpn Acad Ser B: Phys Biol Sci 2005;81:117.
[29] Yamago S. J Polym Sci A: Polym Chem 2006;44:1.
[30] Yamago S. Chem Rev 2009;109:5051.
[31] Yamago S, Nakamura Y. In: Rappoport Z, Marek I, Liebman JF, editors. Patai's chemistry of functional groups, organic selenium and tellurium compounds, vol. 3. Chichester, UK: John Wiley & Sons, Ltd.; 2012. p. 585.
[32] Yamago S, Kayahara E. In: Chatgilialoglu C, Studer A, editors. Encyclopedia of radicals in chemistry, biology & materials. Chichester, UK: John Wiley & Sons Ltd; 2012. p. 1931.
[33] Wayland BB, Poszmik G, Mukerjee SL, Fryd M. J Am Chem Soc 1994;116: 7943.
[34] Debuigne A, Caille JR, Jérôme R. Angew Chem Int Ed 2005;44:1101.
[35] Debuigne A, Poli R, Jérôme C, Jérôme R, Detrembleur C. Prog Polym Sci 2009; 34:211.
[36] Hurtgen M, Detrembleur C, Jerome C, Debuigne A. Polym Rev 2011;51:188.
[37] Asandei AD, Moran IW. J Am Chem Soc 2004;126:15932.
[38] Percec V, Guliashvili T, Ladislaw JS, Wistrand A, Stjemdahl A, Sienkowska MJ, et al. J Am Chem Soc 2006;128:14156.
[39] Rosen B, Percec V. Chem Rev 2009;109:5069.
[40] Oka M, Tatemoto M. Contemporary topics in polymer science. New York: Plenum Press; 1984.
[41] David G, Boyer C, Tonnar J, Ameduri B, Lacroix-Desmazes P, Boutevin B. Chem Rev 2006;106:3936.
[42] Goto A, Tsujii Y, Fukuda T. Polymer 2008;49:5177.
[43] Goto A, Fukuda T. Prog Polym Sci 2004;29:329.
[44] Jenkins AD, Jones RG, Moad G. Pure Appl Chem 2010;82:483.
[45] Fischer H. Chem Rev 2001;101:3581.
[46] Fouassier J-P. Photoinitiation, photopolymerization, and photocuring: fundamentals and applications. Munich: Hanser/Gardner; 1995.
[47] Yagci Y, Jockusch S, Turro NJ. Macromolecules 2010;43:6245.
[48] Otsu T, Yoshida M. Makromol Chem Rapid Commun 1982;3:127.
[49] Otsu T, Yoshida M, Tazaki T. Makromol Chem Rapid Commun 1982;3:133.
[50] Otsu T. J Polym Sci Part A: Polym Chem 2000;38:2121.
[51] Kwon TS, Kumazawa S, Yokoi T, Kondo H, Kunisada H, Yuki Y. J Macromol Sci Pure Appl Chem 1997;A34:1553.
[52] Kwon TS, Kondo S, Kunisada H, Yuki Y. Polym J 1998;30:559.
[53] Kwon TS, Suzuki K, Takagi K, Kunisada H, Yuki Y. J Macromol Sci Pure Appl Chem 2001;A38:591.
[54] Tasdelen MA, Yagci Y. Aust J Chem 2011;64:982.
[55] Tasdelen MA, Çiftci M, Uygun M, Yagci Y. In: Matyjaszewski K, Sumerlin BS, Tsarevsky NV, editors. Progress in controlled radical polymerization materials. Washington, DC: American Chemical Society; 2012. p. p 59.
[56] Benoit D, Chaplinski V, Braslau R, Hawker CJ. J Am Chem Soc 1999;121:3904.
[57] Benoit D, Grimaldi S, Robin S, Finet J-P, Tordo P, Gnanou Y. J Am Chem Soc 2000;122:5929.
[58] Knoop CA, Studer A. J Am Chem Soc 2003;125:16327.
[59] Scaiano JC, Connolly TJ, Mohtat N, Pliva CN. Can J Chem 1997;75:92.
[60] Hu S, Malpert JH, Yang X, Neckers DC. Polymer 2000;41:445.
[61] Ananchenko GS, Fischer H. J Polym Sci Part A: Polym Chem 2001;39:3604.
[62] Goto A, Kwak Y, Yoshikawa C, Tsujii Y, Sugiura Y, Fukuda T. Macromolecules 2002;35:3520.
[63] Goto A, Scaiano JC, Maretti L. Photochem Photobiol Sci 2007;6:833.
[64] Guillaneuf Y, Bertin D, Gigmes D, Versace D-L, Lalevée J, Fouassier J-P. Macromolecules 2010;43:2204.
[65] Jakubowski W, Min K, Matyjaszewski K. Macromolecules 2006;39:39.
[66] Jakubowski W, Matyjaszewski K. Macromolecules 2005;38:4139.
[67] Matyjaszewski K, Jakubowski W, Min K, Tang W, Huang J, Braunecker WA, et al. Proc Natl Acad Sci 2006;103:15309.
[68] Kwiatkowski P, Jurczak J, Pietrasik J, Jakubowski W, Mueller L, Matyjaszewski K. Macromolecules 2008;41:1067.
[69] Magenau AJD, Strandwitz NC, Gennaro A, Matyjaszewski K. Science 2011; 332:81.
[70] Guan Z, Smart B. Macromolecules 2000;33:6904.
[71] Kwak Y, Matyjaszewski K. Macromolecules 2010;43:5180.
[72] Tasdelen MA, Uygun M, Yagci Y. Macromol Rapid Commun 2011;32:58.
[73] Tasdelen MA, Uygun M, Yagci Y. Macromol Chem Phys 2010;211:2271.
[74] Tasdelen MA, Uygun M, Yagci Y. Macromol Chem Phys 2011;212:2036.

[75] Tasdelen MA, Ciftci M, Yagci Y. Macromol Chem Phys 2012;213:1391.
[76] Mosnáček J, Ilčíková M. Macromolecules 2012;45:5859.
[77] Yoon TP, Ischay M, Du J. Nat Chem 2010;2:527.
[78] Narayanam JMR, Stephenson CRJ. Chem Soc Rev 2011;40:102.
[79] Zhang G, Song IY, Ahn KH, Park T, Choi W. Macromolecules 2011;44:7594.
[80] Fors BP, Hawker CJ. Angew Chem Int Ed 2012;51:8850.
[81] Qin S-H, Qin D-Q, Qiu K-Y. New J Chem 2001;25:893.
[82] Bryaskova R, Willet N, Debuigne A, Jérôme R, Detrembleur C. J Polym Sci A: Polym Chem 2007;45:81.
[83] Bryaskova R, Detrembleur C, Debuigne A, Jerome R. Macromolecules 2006; 39:8263.
[84] Debuigne A, Champouret Y, Jerome R, Poli R, Detrembleur C. Chem Eur J 2008;14:4046.
[85] Hurtgen M, Debuigne A, Jérôme C, Detrembleur C. Macromolecules 2010; 43:886.
[86] Detrembleur C, Versace D-L, Piette Y, Hurtgen M, Jérôme C, Lalevée J, et al. Polym Chem 2012;3:1856.
[87] Debuigne A, Schoumacher M, Willet N, Riva R, Zhu X, Rütten S, et al. Chem Commun 2011;47:12703.
[88] Goto A, Sato K, Tsujii Y, Fukuda T, Moad G, Rizzardo E, et al. Macromolecules 2001;34:402.
[89] Goto A, Kwak Y, Fukuda T, Yamago S, Iida K, Nakajima M, et al. J Am Chem Soc 2003;125:8720.
[90] Kwak Y, Goto A, Fukuda T, Kobayashi Y, Yamago S. Macromolecules 2006;39: 4671.
[91] Goto A, Ohno K, Fukuda T. Macromolecules 1998;31:2809.
[92] Kwak Y, Goto A, Fukuda T, Yamago S, Ray B. Z Phys Chem 2005;219:283.
[93] Queffelec J, Gaynor SG, Matyjaszewski K. Macromolecules 2000;33:8629.
[94] Siegenthaler KO, Studer A. Macromolecules 2006;39:1347.
[95] Chong BYK, Le TPT, Moad G, Rizzardo E, Thang SH. Macromolecules 1999;32: 2071.
[96] Nakamura Y, Kitada Y, Kobayashi Y, Ray B, Yamago S. Macromolecules 2011; 44:8388.
[97] Monteiro MJ, de Brouwer H. Macromolecules 2001;34:349.
[98] Kwak Y, Goto A, Tsujii Y, Murata Y, Komatsu K, Fukuda T. Macromolecules 2002;35:3026.
[99] Kwak Y, Goto A, Fukuda T. Macromolecules 2004;37:1219.
[100] Bai R-K, You Y-Z, Pan C-Y. Macromol Rapid Commun 2001;22:315.
[101] Quinn JF, Barner L, Rizzardo E, Davis TP. J Polym Sci Part A: Polym Chem 2002;40:19.
[102] You Y, Hong C, Bai R, Pan C, Wang J. Macromol Chem Phys 2002;203:477.
[103] Quinn JF, Barner L, Barner-Kowollik C, Rizzardo E, Davis TP. Macromolecules 2002;35:7620.
[104] Jiang W, Lu L, Cai Y. Macromol Rapid Commun 2007;27:725.
[105] Chen C, Zhu X, Zhu J, Cheng Z. Macromol Rapid Commun 2004;25:818.
[106] Tasdelen MA, Durmaz YY, Karagoz B, Bicak N, Yagci Y. J Polym Sci A: Polym Chem 2008;46:3387.
[107] Quinn JF, Barner L, Davis TP, Thang SH, Rizzardo E. Macromol Rapid Commun 2002;23:717.
[108] Barner L, Quinn J, Barner-Kowollik C, Vana P, Davis TP. Eur Polym J 2003; 39:449.
[109] Lovestead TM, Hart-Smith G, Davis TP, Stenzel MH, Barner-Kowollik C. Macromolecules 2007;40:4142.
[110] Lu L, Yang N, Cai Y. Chem Commun 2005:5287.
[111] Lu L, Zhang H, Yang N, Cai Y. Macromolecules 2006;39:3770.
[112] Hua D, Bai R, Lu W, Pan C. J Polym Sci Part A: Polym Chem 2004;42:5670.
[113] Hua D, Xiao J, Bai R, Lu W, Pan C. Macromol Chem Phys 2004;205:1793.
[114] Hua D, Ge X, Bai R, Lu W, Pan C. Polymer 2005;46:12696.
[115] Tasdelen MA, Durmaz YY, Karagoz B, Bicak N, Yagci Y. J Polym Sci Part A: Polym Chem 2008;46:3387.
[116] Hong C, You Y, Bai R, Pan C, Borjihan G. J Polym Sci Part A: Polym Chem 2001; 39:3934.
[117] Muthukrishnan S, Pan EH, Stenzel MH, Barner-Kowollik C, Davis TP, Lewis D, et al. Macromolecules 2007;40:2978.
[118] Millard P-E, Barner L, Stenzel M, Davis TP, Barner-Kowollik C, Müller AH. Macromol Rapid Commun 2006;27:821.
[119] Wu D, Hong C, Pan C, He W. Polym Int 2003;52:98.
[120] You Y, Bai R, Pan C. Macromol Chem Phys 2001;202:1980.
[121] Matyjaszewski K, Gaynor S, Wang J-S. Macromolecules 1995;28:2093.
[122] Brimm EO, Lynch MAJ, Sesny WJ. J Am Chem Soc 1954;76:3831.
[123] Koumura K, Satoh K, Kamigaito M. Macromolecules 2008;41:7359.
[124] Collman JP, Hegedus LS, Norton JR, Finke RG. Principles and applications of organotransition metal chemistry. Mill Valley: University Science Books; 1987.
[125] Wakioka M, Baek K-Y, Ando T, Kamigaito M, Sawamoto M. Macromolecules 2002;35:330.
[126] Iovu MC, Matyjaszewski K. Macromolecules 2003;36:9346.
[127] Koumura K, Satoh K, Kamigaito M. J Polym Sci Part A: Polym Chem 2009;47: 1343.
[128] Koumura K, Satoh K, Kamigaito M. Macromolecules 2009;42:2497.
[129] Asandei AD, Adebolu OI, Simpson CP. J Am Chem Soc 2012;134:6080.
[130] http://www.otsukac.co.jp/advanced/living/.
[131] Yamago S, Ukai Y, Matsumoto A, Nakamura Y. J Am Chem Soc 2009;131: 2100.
[132] Mishima E, Yamago S. Macromol Rapid Commun 2011;32:893.
[133] Mishima E, Tamura T, Yamago S. Macromolecules 2012;45:2989.
[134] Mishima E, Yamago S. J Polym Sci A: Polym Chem 2012;50:2254.
[135] Sugihara Y, Kagawa Y, Yamago S, Okubo M. Macromolecules 2007;40:9208.
[136] Mishima E, Tamura T, Yamago S. Macromolecules 2012;45:8998.
[137] Yusa S, Yamago S, Sugahara M, Morikawa S, Yamamoto T, Morishima Y. Macromolecules 2007;40:5907.
[138] Kumar S, Changez M, Murthy CN, Yamago S, Lee J-S. Macromol Rapid Commun 2011;32:1576.
[139] Mishima E, Yamada T, Watanabe H, Yamago S. Chem Asian J 2011;6:445.
[140] Yamada T, Mishima E, Ueki K, Yamago S. Chem Lett 2008:650.
[141] Yamago S, Matsumoto A. J Org Chem 2008;73:7300.
[142] Yamago S, Kayahara E, Yamada H. React Funct Polym 2009;69:416.
[143] Kayahara E, Yamago S. In: Matyjaszewski K, Sumerlin BS, Tsarevsky NV, editors. Progress in controlled radical polymerization materials. Washington, DC: American Chemical Society; 2012. p. 99.
[144] Asua JM, Beuermann S, Buback M, Castignolles P, Charluex B, Gilbert RG, et al. Macromol Chem Phys 2004;205:2151.
[145] Nakamura Y, Arima T, Tomita S, Yamago S. J Am Chem Soc 2012;134:5536.
[146] Yoshikawa C, Goto A, Fukuda T. e-Polymers 2002;13:1.
[147] Yurteri S, Cianga I, Yagci Y. Macromol Chem Phys 2003;204:1771.
[148] Sarbu T, Lin K-Y, Ell J, Siegwart DJ, Spanswick J, Matyjaszewski K. Macromolecules 2004;37:3120.
[149] Debuigne A, Jérôme C, Detrembleur C. Angew Chem Int Ed 2009;48:1422.
[150] Debuigne A, Poli R, Winter JD, Laurent P, Gerbaux P, Wathelet J-P, et al. Macromolecules 2010;43:2801.
[151] Debuigne A, Hurtgen M, Detrembleur C, Jérôme C, Barner-Kowollik C, Junkers T. Prog Polym Sci 2012;37:1004.

Shigeru Yamago received his B.S. and Ph.D in chemistry from Tokyo Institute of Technology in 1986 and in 1991, respectively, as an organic chemist under the supervision of Professor Eiichi Nakamura. During that time, he joined Professor Peter Vollhardt's group at UC Berkeley as a summer student (1988). He became an assistant professor at the same institute in 1991, moved to Kyoto University in 1995 as an assistant professor, Osaka City University in 2003 as full professor, and the current position, Institute for Chemical Research, Kyoto University, in 2006. He was a visiting scientist in Dr. Chryssostomos Chatgilialoglu's group at Consiglio Nazionale delle Ricerche in Bologna (2000). He was a research fellow of the Precursory Research for Embryonic Science and Technology (PRESTO) program in Japan Science and Technology Agency (JST) from 2002 to 2006, and has been a principal investigator for Core Research for Evolutional Science and Technology (CREST) program in JST since 2010. He is a recipient of the Incentive Award in Synthetic Organic Chemistry from the Society of Synthetic Organic Chemistry, Japan in 2001, The Chemical Society of Japan Award for Creative Work in 2010, The Asian Core Program Lectureship Award (Singapore) in 2010, The DIC Functional Materials Award from the Society of Synthetic Organic Chemistry, Japan, in 2012, and The Ichimura Academic Award in 2012.

Yasuyuki Nakamura received his B.S. and Ph.D in chemistry from Kyoto University in 2003 and in 2008, respectively, under the direction of Professor Atsuhiro Osuka. During that time, he joined Professor Michael R. Wasielewski's group at Northwestern University as a short-term visiting student (2006). He was selected as a Research Fellow of the Japan Society for the Promotion of Science in 2005. He started an academic carrier at Institute for Chemical Research, Kyoto University, with Prof. S. Yamago in 2007.